

14. Allevetti, M., Coleman, F. T., Grout, M., Friebe, G. P. & Pier, G. B. Acquisition of expression of the *Pseudomonas aeruginosa* ExoU cytotoxin leads to increased bacterial virulence in a murine model of acute pneumonia and systemic spread. *Infect. Immun.* 68, 3998–4004 (2000).
15. Alexander, C. M. et al. Syndecan-1 is required for Wnt-1-induced mammary tumorigenesis in mice. *Nature Genet.* 25, 329–332 (2000).
16. Rostand, K. S. & Esku, I. D. Cholesterol and cholesterol esters: host receptors for *Pseudomonas aeruginosa* adherence. *J. Biol. Chem.* 268, 24053–24059 (1993).
17. Kato, M. et al. Physiological degradation converts the soluble syndecan-1 ectodomain from an inhibitor to a potent activator of FGF-2. *Nature Med.* 4, 691–697 (1998).
18. Subramanian, S. V., Fitzgerald, M. L. & Bernfield, M. Regulated shedding of syndecan-1 and -4 ectodomains by thrombin and growth factor activation. *J. Biol. Chem.* 272, 14713–14720 (1997).
19. Woods, D. E., Cryz, S. J., Friedman, R. L. & Iglewski, B. H. Contribution of toxin A and elastase to virulence of *Pseudomonas aeruginosa* in chronic lung infections of rats. *Infect. Immun.* 56, 1223–1228 (1982).
20. Blackwood, L. L., Stone, R. M., Iglewski, B. H. & Pennington, J. E. Evaluation of *Pseudomonas aeruginosa* exotoxin A and elastase as virulence factors in acute lung infection. *Infect. Immun.* 59, 198–201 (1983).
21. Huttnet, K. M. & Bevins, C. L. Antimicrobial peptides as mediators of epithelial host defense. *Pediatr. Res.* 45, 785–794 (1999).
22. Bals, R., Weiner, D. J. & Wilson, J. M. The innate immune system in cystic fibrosis lung disease. *J. Clin. Invest.* 103, 303–307 (1999).
23. Kainulainen, V., Wang, H., Schick, C. & Bernfield, M. Syndecans, heparan sulfate proteoglycans, maintain the proteolytic balance of acute wound fluids. *J. Biol. Chem.* 273, 11563–11569 (1998).
24. Belarous, A. et al. Mice lacking neutrophil elastase reveal impaired host defense against Gram negative bacterial sepsis. *Nature Med.* 4, 615–618 (1998).
25. LeVine, A. M. et al. Surfactant protein-A-deficient mice are susceptible to *Pseudomonas aeruginosa* infection. *Am. J. Respir. Cell Mol. Biol.* 19, 700–708 (1998).
26. Crouch, E. C. Collectins and pulmonary host defense. *Am. J. Respir. Cell Mol. Biol.* 19, 177–201 (1998).
27. Kuschert, G. S. V. et al. Glycosaminoglycans interact selectively with chemokines and modulate receptor binding and cellular responses. *Biochemistry* 38, 12959–12968 (1999).
28. Pearson, J. P., Feldman, M., Iglewski, B. H. & Prince, A. *Pseudomonas aeruginosa* cell-to-cell signaling is required for virulence in a model of acute pulmonary infections. *Infect. Immun.* 68, 4331–4334 (2000).
29. Schmidtchen, A., Frick, I. & Björck, L. Dermatan sulphate is released by proteinases of common pathogenic bacteria and inactivates antibacterial alpha-defensin. *Mol. Microbiol.* 39, 708–713 (2001).

Supplementary information is available on Nature's World-Wide Web site (<http://www.nature.com>) or as a paper copy from the London editorial office of Nature.

Acknowledgements

We thank A. Drummond and P. Kincade for the peptide hydroxamate (BB1101) and the Ky 8.2 monoclonal antibody, respectively. This work was supported by the Parker B. Francis Foundation (P.W.P.) and the NIH (G.B.P. and M.B.).

Correspondence and requests for materials should be addressed to M.B. (e-mail: merton.bernfield@ch.harvard.edu) or P.W.P. (email: pwpark@bcm.tmc.edu).

Initiation of a G2/M checkpoint after ultraviolet radiation requires p38 kinase

Dmitry V. Bulavin*, Yuichiro Higashimoto†, Ian J. Popoff‡, William A. Gaardet, Venkatesha Basrurt, Olga Potapova§, Ettore Appella† & Albert J. Fornace Jr*

* Division of Basic Science and † Laboratory of Cell Biology, National Cancer Institute, National Institutes of Health, Bethesda, Maryland 20892, USA

‡ Isis Pharmaceuticals Inc., Carlsbad, California 92008, USA

§ Laboratory of Biological Chemistry, National Institute on Aging, NIH, Baltimore, Maryland 21224, USA

Response to genotoxic stress can be considered as a multistage process involving initiation of cell-cycle arrest and maintenance of arrest during DNA repair¹. Although maintenance of G2/M checkpoints is known to involve Chk1, Chk2/Rad53 and upstream components, the mechanisms involved in its initiation are less well defined^{1–4}. Here we report that p38 kinase has a critical role in the initiation of a G2 delay after ultraviolet radiation. Inhibition of p38 blocks the rapid initiation of this checkpoint in both

human and murine cells after ultraviolet radiation. *In vitro*, p38 binds and phosphorylates Cdc25B at serines 309 and 361, and Cdc25C at serine 216; phosphorylation of these residues is required for binding to 14-3-3 proteins. *In vivo*, inhibition of p38 prevents both phosphorylation of Cdc25B at serine 309 and 14-3-3 binding after ultraviolet radiation, and mutation of this site is sufficient to inhibit the checkpoint initiation. In contrast, *in vivo* Cdc25C binding to 14-3-3 is not affected by p38 inhibition after ultraviolet radiation. We propose that regulation of Cdc25B phosphorylation by p38 is a critical event for initiating the G2/M checkpoint after ultraviolet radiation.

Evidence exists for important differences in the induction of G2/M delays after DNA strand damage caused by ionizing radiation (IR) and ultraviolet (UV) radiation^{1,5}. Several mechanisms are involved in regulating G2/M delay after IR, and a key component includes activation of Chk1 and Chk2 by the cell cycle proteins ATM and/or ATR, which results in phosphorylation of Cdc25C at Ser 216 (refs 1, 2, 6, 7). Less is known about checkpoint regulation after UV radiation, but evidence indicates that Cdc25 may be involved^{1,7,8}, whereas ATM seems to be involved primarily in IR- rather than UV-induced damage signalling¹. After either IR or UV radiation the initiation of the G2/M checkpoint is rapid, but the regulation of these early events has not been well characterized. Cdc25B, a cytoplasmic protein in G2/M⁹, has been termed a 'starter protein' for G2/M progression as it is activated before Cdc25C^{7,10}; thus, Cdc25B is a candidate for G2 checkpoint initiation.

The mitogen-activated protein kinase (MAPK) pathway has a central role in cellular signalling and two of its three components, the p38 kinase and Jun amino-terminal kinase (JNK), are activated rapidly by many stresses including UV radiation. To address the potential role of p38 kinase in the regulation of cell-cycle progression, we determined the effect of a specific p38 inhibitor (SB202190) on UV-induced checkpoint activation. Whereas inhibition of p38 had no discernible effect on G1 checkpoint activation as measured by progression into S phase (data not shown), the rapid onset of G2 checkpoint was strongly inhibited. For primary isogenic cells from wild-type, p53^{-/-} and p21^{-/-} mice, the onset of G2 checkpoint was inhibited markedly at both low and high UV radiation doses (Fig. 1a); the only exception was weaker but significant ($P < 0.05$) inhibition in p53^{-/-} cells at the lower dose.

G2 checkpoint activation was measured by the reduction in the mitotic index at early times after irradiation³; the duration of G2/M in these dermal fibroblasts was estimated to be about 4.5 h, and thus excluded a contribution by UV-induced S-phase delay during the first 4 h. Using 20 J m⁻², inhibition was also seen in p53 wild-type and p53-deficient human tumour lines including HeLa cells (Fig. 2b). Treatment with SB202190 reduced p38 activity in all three types of dermal fibroblast, as determined by phosphorylation of glutathione S-transferase (GST)-ATF2, whereas it had no effect on JNK activity, as measured by GST-Jun phosphorylation (Fig. 1a). Neither the inhibitor nor UV radiation affected the level of cellular p38 (data not shown). Notably, changes in the mitotic index correlated with Cdc2 kinase activity, as measured by phosphorylation of histone H1 (Fig. 1a, HH1). Ultraviolet radiation decreased Cdc2 kinase activity in all cell lines tested, and p38 inhibition completely blocked the decrease during the first hours after irradiation.

The role for p38 in the control of G2 progression seems to be specific for particular types of stress, as it affected neither IR-induced checkpoint activation nor normal G2/M progression. Ionizing radiation frequently does not induce appreciable activation of MAPKs including p38 (ref. 11), and the p38 inhibitor had no effect on the rapid onset of G2 checkpoint in either wild-type or p53-deficient cells (Fig. 1b). Moreover, inhibitors of IR signalling proteins, such as caffeine (ATM/ATR) and UCN-01 (Chk1), had no effect on the initiation of the UV-induced G2 checkpoint (Fig. 2b). In non-irradiated cells, inhibition of p38 also had no detectable

effect on normal G2/M progression (Fig. 1c).

The p38-mediated G2 checkpoint occurs in p53-deficient cells, but seemed to be attenuated at the lower UV dose (Fig. 1a). As higher doses triggered strong activation of the p38-dependent checkpoint regardless of p53 status, we carried out further studies in p53-deficient HeLa cells. HeLa cells express only two of the four isoforms of p38 at appreciable levels¹²; both p38 α and p38 β are strongly inhibited by SB202190, whereas the other two p38 isoforms are not¹³. We could selectively block these two p38 isoforms, which are ubiquitously expressed in most cell types, with an antisense oligonucleotide approach (Fig. 2a) that also attenuated UV-induced checkpoint activation. Suppression of either p38 α or p38 β levels interfered with normal UV checkpoint activation with slightly different kinetics (Fig. 2b). The p38 α oligonucleotide could reduce G2 arrest to that achieved with SB202190, whereas inhibition of p38 β had a more transient effect with prominent attenuation only in the first hour after irradiation. These results support a role for both p38 isoforms in checkpoint activation.

We attempted to identify the p38 substrate(s) involved in G2 checkpoint control. Previous studies have indicated that a peptide containing an LSP motif is a substrate for p38, and this motif can be found in many proteins including the cell-cycle control proteins p53 (Ser33 and Ser46)¹⁴, cyclin B1 (Ser116), Myt1 (Ser431) and

Cdc25B (Ser15, Ser224, Ser235). Mutation of Ser116 had no effect on cyclin B1 localization or on Cdc2/cyclin B1 kinase activity (data not shown). Likewise, mutation of Ser431 to alanine in Myt1 did not affect its ability to inhibit Cdc2 kinase activity, nor did it affect the ability of Myt1 to sequester either wild-type or S116A cyclin B1 in the cytoplasm when nuclear export of cyclin B1 was interrupted by leptomycin B (data not shown). Ultraviolet radiation did not affect the cellular localization or protein level of Cdc25B (data not shown). In contrast, it has been shown that incubating Cdc2 complex from UV-irradiated cells with GST-Cdc25B is sufficient to restore Cdc2 activity¹⁵, indicating that Cdc2 phosphorylation is a more likely target for G2 control after UV radiation.

Cdc25B activity is essential for G2/M transition¹⁶ and has been implicated in the regulation of Cdc2 activity after UV radiation⁴. Consequently, we synthesized peptides corresponding to regions containing the LSP motif, as well as to the 14-3-3-binding region (303–312), and incubated them with p38 α -Flag isolated from UV-irradiated cells¹⁴. Unexpectedly, p38 α phosphorylated the 14-3-3-binding region at least 25 times more efficiently than the LSP peptides (Fig. 3a, lanes 1–4). We next used peptides that matched the consensus 14-3-3-binding sites¹⁶ (RSXpSXP or RXY/FXpSXP) in Cdc25B (containing Ser137, Ser216, Ser309 and Ser361) and

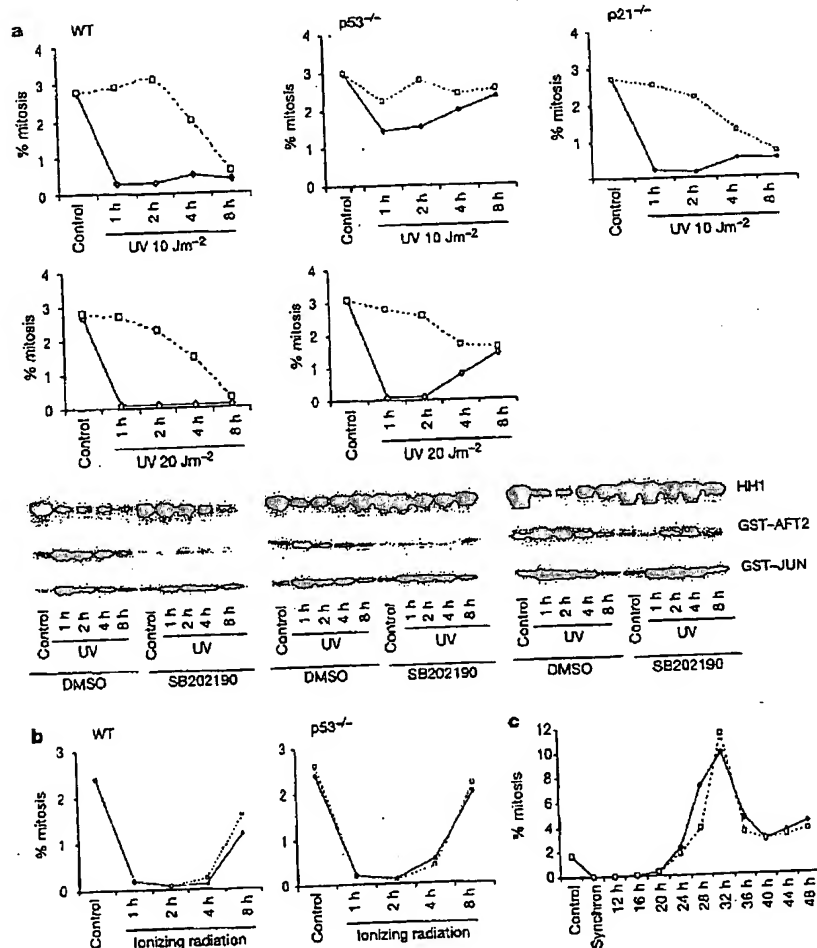
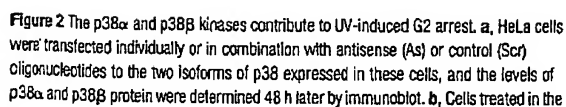


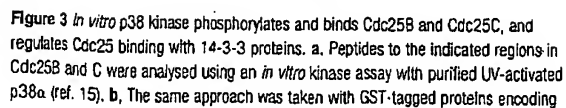
Figure 1 A principal role for p38 kinase in G2 checkpoint activation after UV radiation. **a**, Dermal fibroblasts (DFs) established from wild-type, p53^{-/-} and p21^{-/-} mice were UV irradiated in the presence of 10 μ M p38 inhibitor SB202190 (open symbols) or dimethyl sulfoxide (DMSO; filled symbols) as a control, and the percentage of cells in mitosis and Cdc2, p38 and JNK activities were determined. **b**, Wild-type and p53^{-/-} DFs were

γ -irradiated (3 Gy) in the presence of SB202190 or DMSO and the mitotic indexes were determined as in **a**. **c**, Wild-type DFs were synchronized with 0.25% serum for 3 d, and then stimulated with 20% serum. SB202190 or DMSO was added 20 h later and the mitotic index was determined.

BEST AVAILABLE COPY



same manner were UV-irradiated with 20 J m^{-2} 48 h after transfection, and the mitotic index was determined at the indicated times following irradiation. Top left, SB202190, caffeine and UCN-01 were added 0.5 h before irradiation.



either wild-type or the designated mutant of Cdc25B and Cdc25C. **c**, Association of p38 α kinase with Cdc25B and Cdc25C. **d**, Association of p38-phosphorylated Cdc25 with 14-3-3 was analysed as described in Methods.

Cdc25C (containing Ser 216). All these sites, with the exception of Cdc25B Ser 216, were phosphorylated (Fig. 3a).

We extended these experiments to whole proteins and found that mutation of Ser 216 in Cdc25C or the combination of Ser 309/Ser 361 in Cdc25B reduced phosphorylation by p38 to about 10% of that in the wild-type protein (Fig. 3b). Mutation at Ser 137 either alone or in combination with Ser 309 or Ser 361 had no appreciable effect, and thus we conclude that Ser 309/Ser 361 in Cdc25B and Ser 216 in Cdc25C are the most critical sites for phosphorylation by p38 α and p38 β (data not shown) kinases.

To determine whether p38 kinase and the Cdc25 proteins form a complex, GST-Cdc25C and GST-Cdc25B bound to glutathione beads were incubated with cell extracts from HeLa cells and precipitated. Both fusion proteins bound p38 kinase specifically, whereas GST alone did not (Fig. 3c), indicating the presence of a complex. Notably, mutation of the phosphorylation sites on both proteins, as well as UV irradiation of HeLa cells, did not affect binding with p38 kinase (data not shown).

Phosphorylation of Cdc25 triggers cell-cycle arrest by the sequestration of Cdc25 by 14-3-3 (refs 1, 17, 18). We found that phosphorylation of Cdc25B or Cdc25C by p38 kinase results in a significant increase of 14-3-3 binding (Fig. 3d). For Cdc25C, this increased binding was primarily dependent on phosphorylation of Ser 216, because mutation of this site significantly reduced p38-kinase-induced binding to 14-3-3 proteins. For Cdc25B, mutation of either Ser 309 or Ser 361 alone was sufficient to reduce 14-3-3 binding to that observed with the S309A/S361A double mutant (Fig. 3d); this indicates that phosphorylation at both sites is required for strong p38-kinase-induced binding.

Both Cdc25B and Cdc25C bound to 14-3-3 under normal

conditions *in vivo* and inhibition of p38 did not affect this binding, whereas mutation of Ser 309 in Cdc25B or Ser 216 in Cdc25C to alanine decreased complex formation (Fig. 4a). Ultraviolet radiation had no significant effect on 14-3-3 binding, nor did inactivation of p38 change complex formation with Cdc25C after UV radiation. For Cdc25B, however, 14-3-3 binding was significantly reduced in UV-irradiated cells after p38 inactivation (Fig. 4a). These results support an important role for p38 in the regulation of Cdc25B by 14-3-3 after stresses such as UV radiation, but argue against a significant role in the regulation of Cdc25C.

To address further the *in vivo* role for p38 kinase in regulating phosphorylation of Cdc25B Ser 309, we generated a phospho-specific antibody to this site. Analysis of non-synchronized HeLa cells showed that this site is phosphorylated in non-synchronized cells as well as in G1, S and G2 phases of the cell cycle (Fig. 4b). In mitosis, however, Cdc25B phosphorylation at Ser 309 was reduced markedly, correlating with high Cdc25B phosphatase activity (Fig. 4b, bottom panel). Ultraviolet radiation had no effect on Cdc25B phosphorylation at Ser 309, and inactivation of p38 kinase did not affect Ser 309 phosphorylation in control cells, but this phosphorylation was significantly reduced in asynchronous UV-irradiated cells in the presence of the p38 inhibitor (Fig. 4c).

We investigated the role of Cdc25B Ser 309 in regulating the initiation of G2 checkpoint. Synchronized HeLa cells were transfected with different green fluorescent protein (GFP) fusion constructs, and progression through G2 phase was analysed (Fig. 4d). Under these conditions, cells entered mitosis 8–9 h after release in complete medium and only 3% of the GFP-positive cells could reach mitosis by 7 h (Fig. 4d). As overexpression of wild-type Cdc25B induces premature onset of mitosis (Fig. 4b)⁹, the cells were UV

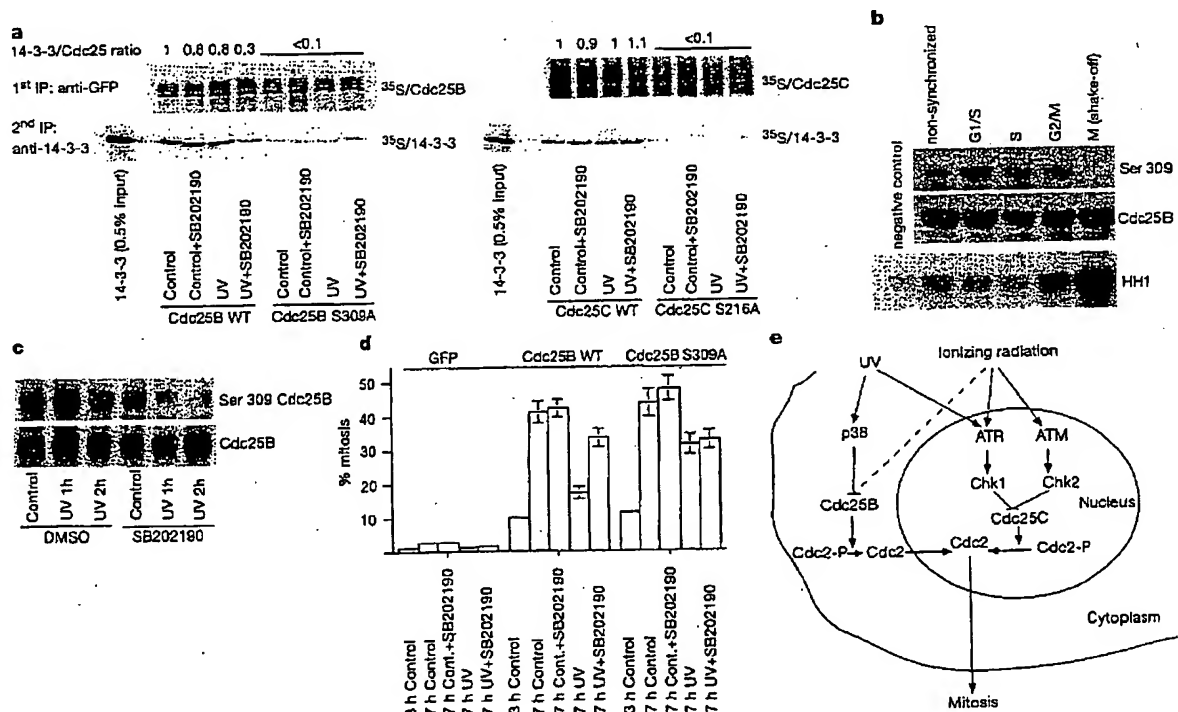


Figure 4 *In vivo* phosphorylation of Ser 309 Cdc25B after UV radiation, and its role in regulating 14-3-3 binding and G2/M checkpoint control. **a**, The level of 14-3-3 in complex with Cdc25 *in vivo* was determined after sequential immunoprecipitations (see Methods). **b**, Ser 309 Cdc25B phosphorylation and Cdc25B activity (bottom panel) were analysed at the different phases of the cell cycle. **c**, HeLa cells were treated with DMSO or SB202190 (20 μ M) and UV irradiated (20 J m⁻²) after 30 min; Ser 309 Cdc25B phosphorylation was then analysed. **d**, In cell synchrony experiments, cells were

transfected with the indicated GFP fusion plasmids (see Methods). Cells, which had progressed past G2 phase, were arrested in mitosis with nocodazole over the next 4 h (7 h control, unirradiated samples; 7 h control + SB202190, unirradiated samples in the presence of p38 inhibitor; 7 h UV, UV-irradiated cells; 7 h UV + SB202190, UV-irradiated cells in the presence of the p38 inhibitor). The number of GFP-positive cells in mitosis was counted. **e**, A model for the role of p38 kinase in regulating G2/M checkpoint activation after genotoxic stress. Dotted line refers to unidentified, activated kinase.

irradiated only 3 h after release in complete medium. Ultraviolet radiation abrogated G2 progression in Cdc25B wild-type GFP-positive cells, and the p38 inhibitor could overcome this checkpoint. The Cdc25B S309A mutant also induced premature entry into mitosis, but UV radiation had much less effect on G2 progression, and inclusion of the p38 inhibitor had no significant effect on G2 progression after UV radiation (Fig. 4d). These data show that abrogation of Cdc25B Ser 309 phosphorylation is sufficient to overcome initiation of the G2 checkpoint after UV radiation, and that this site is a critical target for p38 kinase in its regulation of checkpoint initiation.

Before mitosis, Cdc25B and Cdc25C are phosphorylated at Ser 309 and Ser 216, respectively, with resultant complex formation with 14-3-3 proteins. Maintaining this phosphorylation *in vivo* must involve one or more kinases, which regulate entry into mitosis under normal (non-stress) conditions, although the specific kinases and how their activities are controlled remain uncertain. After genotoxic stress Cdc25 phosphorylation is required to prevent progression into mitosis, but the exact mechanism has not been certain because these inhibitory sites are already phosphorylated in G2 phase, even in unstressed cells.

On the basis of our results and data for Chk1-dependent phosphorylation of Cdc25C after IR¹⁹, a model can be proposed for the activation of the G2 checkpoint (Fig. 4e). After genotoxic stress, cells activate a mechanism that switches the system of kinases regulating Cdc25 phosphorylation in unstressed cells to kinases that are stress-inducible. By switching kinases after stress, the cell creates a system that becomes 'a sensor' for damage and allows entry to mitosis only after appropriate stress recovery. In this case, p38 kinase is an early 'sensor' of cell damage because it regulates Cdc25B phosphorylation (Fig. 4c). Later events in the maintenance of G2 arrest involve other components (such as ATR/ATM pathways) that participate in regulating Cdc25C in the nucleus and can be induced by most stresses including UV radiation as well as IR. For example, disruption of either the Chk1 or Chk2 genes attenuated only the later time points (12 h and later) but not the initiation of the UV or IR G2/M checkpoints^{4,20}. It is striking that both initiation and maintenance pathways target the same system of Cdc25 phosphatases, emphasizing their central role in the regulation of G2/M progression after genotoxic stress.

Note added in proof: It has recently been shown that a yeast analogue of p38 kinase, HOG1, is required for hypertonic stress-induced G2 arrest²¹.

Methods

Plasmids and site-directed mutagenesis

p38 α and p38 β expression vectors were obtained from R. Davis and J. Han, respectively. GST-Cdc25B and GST-Cdc25C plasmids were provided by L. Hoffmann and H. Piwnicka-Worms. We obtained GFP-Cdc25B and GFP-Cdc25C from J. Pines. To generate site mutants, we used a site-directed mutagenesis kit (Stratagene) with the following pairs of primers: for Cdc25B S137A, 5'-cagacgttccaggtatgcccgtgagctgc-3'/5'-gcagccctacggcatgctcgtgagcagctg-3'; S309A, 5'-cggtcttccgtctcgcgcacgtccctcag-3'/5'-ctcagggcagggcggagcggagagcgcg-3'; S361A, 5'-gtctccgcctcaaaagcactgtgtcagcatgag-3'/5'-ctatcgtgacacagtgctttttagcggagac-3'; and for Cdc25C S216A, 5'-ccctatctcgtcccgccgagatgcagagac-3'/5'-gtctctggtcgtcgcgggagcagatagc-3'. Results were verified by DNA sequencing.

Analysis of protein binding

Bacterially expressed GST proteins (GST, GST-Cdc25B, GST-Cdc25C or the indicated mutants) on glutathione beads were incubated overnight with protein extracts from HeLa cells (1 mg) and precipitated. p38 α was analysed by C-20, and p38 β by C-16 polyclonal antibodies (Santa Cruz). To analyse 14-3-3 binding, GST proteins were phosphorylated for 1 h with UV-activated p38 α (ref. 15); we used a UVC radiation source for all experiments. 14-3-3 proteins in complex with GST proteins were analysed by immunoblotting with polyclonal antibody (K-19, Santa Cruz). For analysis of Cdc25 interaction with 14-3-3 proteins, HeLa cells were co-transfected with 5 μ g of GFP-tagged Cdc25 plasmids and 5 μ g of haemagglutinin A (HA)-tagged 14-3-3. On the next day, cells were labelled with 300 μ Ci [³⁵S]methionine per ml of EasyTag Express Protein Labeling Mix (NEN) for 60 min and then UV irradiated (60 J m⁻²). For some samples, we added 40 μ M SB202190 30 min before UV radiation to block p38 activity. Labelling was continued for

the next 60 min, and the cells were gathered. Cdc25s were precipitated with anti-GFP antibody. After boiling in SDS sample buffer, precipitates were diluted 30 times with lysis buffer, and 14-3-3 was subsequently re-immunoprecipitated with 10 μ l of anti 14-3-3 antibody (Santa Cruz) and 5 μ l of anti-HA antibody (Rabco).

Kinase and phosphatase assays

The p38 and Cdc2 kinase assays were performed after immunoprecipitation with specific antibodies^{14,21} using GST-ATF2 and histone H1, respectively. We analysed JNK kinase after pull down with GST-Jun. Cdc25B activity was determined after dephosphorylation of Cdc2, with subsequent analysis of Cdc2 activity using histone H1 as a substrate²¹.

Analysis of the role of Ser 309 Cdc25B

HeLa cells were synchronized by a double-thymidine block procedure as described²². Two hours before the second incubation with thymidine, we transfected the cells with the indicated GFP fusion plasmids (Fig. 4d). Cells were irradiated 3 h after release into complete medium with 20 J m⁻², and nocodazole was added during the next 4 h to trap any cells that had progressed through G2 into mitosis. We determined the number of GFP-positive cells in mitosis as described⁴. Mitotic cells were obtained by a mitotic shake-off procedure; cells were collected at 8 h after release from the double-thymidine block, when the fraction of G2/M cells was maximal as determined by FACS, and then every 45 min thereafter during the next 2.25 h.

Analysis of phosphorylation

Ser 216 Cdc25C antibody was from Cell Signaling Technology. Rabbit polyclonal antibody specific for phosphorylation at Ser 309 Cdc25B was raised against the sequence Ac-305-314(309P) (that is, Ac-FRSFSP(P)-MPCSV) conjugated to keyhole limpet haemocyanin. We confirmed the specificity of antibody by enzyme-linked immunosorbent and immunoblot assays with GST proteins.

Oligonucleotide synthesis and treatment

The 20-nucleotide oligonucleotides used in this study were synthesized at ISIS Pharmaceuticals Inc. as follows: p38 α antisense, 5'-ttctctatctgagccaa-3'; p38 α scrambled, 5'-ttatctcagcttagacctat-3'; p38 β antisense, 5'-gtactgtctgcgcgtgga-3'; p38 β scrambled, 5'-gtctcagctgcgtgtcga-3'. All oligonucleotides contained five 2'-O-methoxyethyl-modified sugar/phosphodiester residues at the 5' and 3' ends, flanking the centre ten 2'-deoxyoligonucleotide/phosphorothioate residues. Cells were treated with 0.3 μ M oligonucleotides in the presence of 10 μ g ml⁻¹ of Lipofectin reagent (Life Technologies).

Received 4 December 2000; accepted 23 February 2001.

1. Pines, J. Four-dimensional control of the cell cycle. *Nature Cell Biol.* 1, E73–E79 (1999).
2. Peng, C. Y. et al. Mitotic and G2 checkpoint control: regulation of 14-3-3 protein binding by phosphorylation of Cdc25C on serine-216. *Science* 277, 1501–1505 (1997).
3. Furnari, B., Rhind, N. & Russell, P. Cdc25 mitotic inducer targeted by chk1 DNA damage checkpoint kinase. *Science* 277, 1495–1497 (1997).
4. Hirao, A. et al. DNA damage-induced activation of p53 by the checkpoint kinase Chk2. *Science* 287, 1824–1827 (2000).
5. Hollander, M. C. et al. Genomic instability in *Cadd45a*-deficient mice. *Nature Genet.* 23, 176–184 (1999).
6. Sanchez, Y. et al. Conservation of the Chk1 checkpoint pathway in mammals: linkage of DNA damage to Cdk regulation through Cdc25. *Science* 277, 1497–1501 (1997).
7. Nilsson, I. & Hoffmann, J. Cell cycle regulation by the Cdc25 phosphatase family. *Prog. Cell Cycle Res.* 4, 107–114 (2000).
8. Gabrielli, B. G., Clark, J. M., McCormack, A. K. & Ellem, K. A. Ultraviolet light-induced G2 phase cell cycle checkpoint blocks cdc25- dependent progression into mitosis. *Oncogene* 15, 749–758 (1997).
9. Karlsson, C., Katich, S., Hagring, A., Hoffmann, J. & Pines, J. Cdc25B and Cdc25C differ markedly in their properties as initiators of mitosis. *J. Cell Biol.* 146, 573–584 (1999).
10. Lammier, C. et al. The Cdc25B phosphatase is essential for the G2/M phase transition in human cells. *J. Cell Sci.* 111, 2445–2453 (1998).
11. Liu, Z. G. et al. Three distinct signalling responses by murine fibroblasts to genotoxic stress. *Nature* 384, 273–276 (1996).
12. Jiang, Y. et al. Characterization of the structure and function of the fourth member of p38 group mitogen-activated protein kinases, p38 δ . *J. Biol. Chem.* 272, 30122–30128 (1997).
13. Lee, J. C., Kazanietz, S., Kumar, S., Badger, A. & Adams, J. L. p38 mitogen-activated protein kinase inhibitors—mechanisms and therapeutic potentials. *Pharmacol. Ther.* 82, 389–397 (1999).
14. Bulavin, D. et al. Phosphorylation of human p53 by p38 kinase coordinates N-terminal phosphorylation and apoptosis in response to UV radiation. *EMBO J.* 18, 6845–6854 (1999).
15. Poon, R. Y. C., Jiang, W., Toyoshima, M. & Hunter, T. Cyclin-dependent kinases are inactivated by a combination of p21 and Thr-147/Tyr-15 phosphorylation after UV-induced DNA damage. *J. Biol. Chem.* 271, 13283–13291 (1996).
16. Yaffe, M. B. et al. The structural basis for 14-3-3:phosphopeptide binding specificity. *Cell* 91, 961–971 (1997).
17. Lopez-Girona, A., Furnari, B., Mondesert, O. & Russell, P. Nuclear localization of Cdc25 is regulated by DNA damage and a 14-3-3 protein. *Nature* 397, 172–175 (1999).
18. Morris, M. C., Heitz, A., Mery, J., Heitz, R. & Divita, G. B. An essential phosphorylation-site domain of human CDC25C interacts with both 14-3-3 and cyclins. *J. Biol. Chem.* 275, 28849–28857 (2000).
19. Graves, P. R. et al. The Chk1 protein kinase and the Cdc25C regulatory pathways are targets of the anticancer agent UCN-01. *J. Biol. Chem.* 275, 5600–5603 (2000).
20. Liu, Q. et al. Chk1 is an essential kinase that is regulated by Atr and required for the G2/M DNA damage checkpoint. *Genes Dev.* 14, 1448–1459 (2000).

21. Blasina, A. *et al.* A human homologue of the checkpoint kinase Cds1 directly inhibits Cdc25 phosphatase. *Curr. Biol.* 9, 1–10 (1999).
22. Liu, F., Rothblum-Ovniati, C., Ryan, C. E. & Piwnicka-Worms, H. Overproduction of human Myt1 kinase induces a G2 cell cycle delay by interfering with the intracellular trafficking of Cdc2-cyclin B1 complexes. *Mol. Cell. Biol.* 19, 5113–5123 (1999).
23. Alexander, M. R. *et al.* Regulation of cell cycle progression by swp1 and hng1p following hypertonic stress. *Mol. Biol. Cell* 12, 53–62 (2001).

Supplementary information is available on Nature's World-Wide Web site (<http://www.nature.com>) or as paper copy from the London editorial office of Nature.

Acknowledgements

We are grateful to J. Pines, J. Hoffmann, H. Piwnicka-Worms, J. Han, B. Vogelstein and R. Davis for the plasmids used in the paper; D. Ferris for Cdc2 polyclonal antibody; B. Monia for advice on the antisense oligonucleotide approach; J. Clark for help with DNA sequencing; and O. Kovalsky for help in protein isolation.

Correspondence and requests for materials should be addressed to A.J.F. (e-mail: formace@nih.gov).

Microarrays of cells expressing defined cDNAs

Junaid Ziauddin & David M. Sabatini

Whitehead Institute for Biomedical Research, 9 Cambridge Center, Cambridge, Massachusetts 02142, USA

Genome and expressed sequence tag projects are rapidly cataloguing and cloning the genes of higher organisms, including humans. An emerging challenge is to rapidly uncover the functions of genes and to identify gene products with desired properties. We have developed a microarray-driven gene expression system for the functional analysis of many gene products in parallel. Mammalian cells are cultured on a glass slide printed in defined locations with different DNAs. Cells growing on the printed areas take up the DNA, creating spots of localized transfection within a lawn of non-transfected cells. By printing sets of complementary DNAs cloned in expression vectors, we make microarrays whose features are clusters of live cells that express a defined cDNA at each location. Here we demonstrate two uses for our approach: as an alternative to protein microarrays for the identification of drug targets, and as an expression cloning system for the discovery of gene products that alter cellular physiology. By screening transfected cell microarrays expressing 192 different cDNAs, we identified proteins involved in tyrosine kinase signalling, apoptosis and cell adhesion, and with distinct subcellular distributions.

The growing collection of gene sequences and cloned cDNAs demands the development of systematic and high-throughput approaches to characterizing the gene products. Strategies comparable to DNA microarrays for transcriptional profiling^{1,2} and to yeast two-hybrid arrays for determining protein–protein interactions³ do not exist to analyse the function, within mammalian cells, of large sets of genes. At present, *in vivo* gene analysis can be done—on a gene-by-gene scale—by expressing a DNA construct within cells that directs the overproduction of a gene product or inhibits its synthesis or function. The effects on cellular physiology of altering the level of a gene product is then detected using a variety of functional assays. We describe a strategy for the high-throughput analysis of gene function in mammalian cells. We have developed a system suitable for rapidly screening large sets of cDNAs or DNA constructs for those genes encoding desired products or causing cellular phenotypes of interest. Using slides printed with sets of cDNAs in expression vectors, we create living microarrays of cell clusters expressing the gene products. The cell clusters can be

screened for any properly detectable on a surface and the identity of the responsible cDNA determined from the coordinates of the cell cluster with a phenotype of interest.

To create these microarrays, we simultaneously transfect distinct and defined areas of a lawn of cells with different plasmid DNAs (Fig. 1a). This is done without the use of individual wells to sequester the DNAs. Nanolitre volumes of plasmid DNA in an aqueous gelatin solution are printed on a glass slide using a robotic arrayer. After drying, the DNA spots are briefly exposed to a lipid transfection reagent; the slide is then placed in a culture dish and covered with adherent mammalian cells in medium. The cells growing on the DNA and gelatin spots express the DNA and divide 2–3 times in the process of creating a microarray with features consisting of clusters of transfected cells (which we call 'transfected cell microarrays'). We call the method to make the arrays 'reverse transfection' because, compared with conventional transfection, we have reversed the order of addition of DNA and adherent cells. For detailed protocols of this and alternative methods see http://staffa.wi.mit.edu/sabatini_public/reverse_transfection.htm.

To illustrate the method, we printed an array with elements containing an expression construct for the green fluorescent protein (GFP). HEK293 cells were plated on the slide for transfection and the fluorescence of the cells detected with a laser fluorescence scanner. A low magnification scan shows a regular pattern of fluorescent spots that matches the pattern in which we printed the GFP expression construct (Fig. 1b). A higher magnification image obtained through fluorescence microscopy shows that each spot is about 120–150 μm in diameter and consists of a cluster of 30–80 fluorescent cells (Fig. 1c). As in a conventional transfection, the total expression level in the clusters is proportional over a

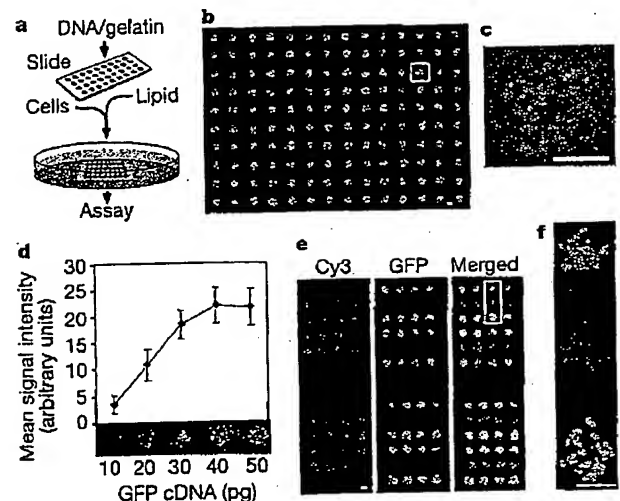


Figure 1 Well-less transfection of plasmid DNAs in defined areas of a lawn of mammalian cells. **a**, Protocol for making microarrays of transfected cells. **b**, Laser scan image of a GFP-expressing microarray made from a slide printed in a 14 × 10 pattern with a GFP expression construct. **c**, Higher magnification image obtained with fluorescence microscopy of the cell cluster boxed in **b**. Scale bar, 100 μm . **d**, Expression levels of cell clusters in a microarray are proportional, over a fourfold range, to the amount of plasmid DNA printed on the slide. Indicated amounts of the GFP construct assume a 1-nl printing volume. The graph shows the mean \pm s.d. of the fluorescence intensities of the cell clusters ($n = 6$). The fluorescent image is from a representative experiment. **e**, Co-transfection is possible with transfected cell microarrays. Arrays with elements containing expression constructs for HA–GST, GFP or both were transfected and processed for immunofluorescence and imaged with a laser scanner. Cy3, cell clusters expressing HA–GST; GFP, cell clusters expressing GFP; merged, superimposition of Cy3 and GFP signals. Yellow colour indicates co-expression. Scale bar, 100 μm . **f**, Enlarged view of boxed area of scan image from **e**.